



POLITECNICO
DI TORINO



INTERNATIONAL MASTER COURSE
PHYSICS OF COMPLEX SYSTEMS

Master PCS Internship Thesis

Active matter and collective motion

Evelyn Camacho Soberón

Experimental report
Advisor: **Alessandro Pelizzola**
Coadvisor: **Denis Bartolo**

March, 2020

*Para mamá.
Estarías orgullosa, siempre y bajo cualquier circunstancia.*

Acknowledgements

Me gustaría agradecer al Politecnico di Torino por la oportunidad en estos dos años de maestría en donde he aprendido y viajado tanto, haciendo ciencia en dos países tan hermosos como lo son Italia y Francia. Agradezco al profesor Mouhanna y al profesor Braunstein por el apoyo brindado, la escucha, la comprensión y el aliento para seguir adelante a pesar de las adversidades. Quiero dar un agradecimiento especial al profesor Alessandro Pelizzola por el asesoramiento, tan importante para mí, al inicio y al final de este camino.

Tampoco sé qué hubiera hecho sin el soporte y la amistad de mis compañeros del PCS. Todo el grupo en estos años me ha mostrado un apoyo invaluable que considero uno de mis tesoros más grandes y nos hemos hecho amigos para toda una vida. Gracias a todos, me han hecho sentir una italiana más en el grupo siempre, con sus brazos abiertos y las charlas calurosas. Serán todos grandes científicos, pero también grandes personas.

Un agradecimiento al Laboratoire de Physique de la ENS de Lyon y a las personas que conocí en el Bartolo team durante estos meses por su bienvenida y ayuda en las circunstancias más difíciles. Todo mi agradecimiento a Amélie y Delphine por su enorme apoyo en la manipulación y manejo del sistema experimental y su paciencia con mis preguntas infinitas sobre el programa de Matlab, siempre fueron extraordinariamente accesibles y estuvieron dispuestas a ayudarme con la mejor de las actitudes y con las sonrisas más grandes, siempre disponibles y positivas. Quisiera también agradecer infinitamente a Marine, por el gigantesco apoyo brindado en el momento más difícil de mi vida y cuando más necesité ayuda para volver a mi país, nunca olvidaré tu lado tan humano y noble. Son un equipo extraordinario y estoy muy feliz de haber vivido la experiencia de trabajar con ustedes.

Gracias particularmente a Denis por permitirme realizar este internship con su equipo, por su paciencia, sus enseñanzas, su apoyo incondicional en todos los sentidos posibles y por darme la oportunidad de aprender tanto en estos meses. Gracias por no dejarme sola y alentarme a seguir adelante y esforzarme con mi trabajo como científica.

Finalmente, gracias infinitas a mis amigos infinitos. A la gente que nunca me deja sola y que llevo siempre a todos lados. La fortuna de mi vida la mido en ustedes, demostrándome siempre que los verdaderos amigos no ven distancias ni circunstancias. A Emilia, Pamela, Des, Aurora, Ana, Donato, Darío, Carlos, Julia, Ale, Dani, Meli, Tats. A mi hermano Peter por ser siempre el mejor amigo. Ustedes son mi familia. A papá, porque ¿acaso falta decirlo? Eres mi superhéroe.

Abstract

Active matter and collective motion

In this report we are interested in the collective motion evolution of self-propelled synthetic particles in a microfluidic circular chamber. We have worked with an experimental model that motorizes colloids of 5 and 10 μm and we have studied the flocking dynamics according to the variation of the density ρ_0 injected in the chamber, which is taken as the control parameter of the system. The colloids experience a transition between a low-density and a high-density phase, in which the interactions of particles velocities leads to the emergence of collective motion and the formation of a vortex inside the circular chamber. We were able to show the phase diagram of the transition correspondent to this system from the experimental results obtained.

The reader will find an overview of the current state of knowledge in the field, as well as a presentation of the actual model experience. The results presented include the velocities histograms of particles and the qualitative comparison between the gas and polar liquid phase. It is also shown the variation of the colloids velocity with respect to the electric field and its linear relation seen through experimentation.

Finally, the description of the construction of the phase diagram and the characterization of the possible states of the system makes it possible to better understand the emergence of the collective motion of flocking in a microfluidic environment.

Contents

Acknowledgments	v
Abstract	vii
Contents	ix
1 Introduction	1
1.1 Objective	1
1.2 Context and framework	2
1.3 Research Plan	8
2 Materials and Methods	9
2.1 Colloidal rollers motorization principles	9
2.2 Motorizing, Handling & Observing colloidal particles	11
2.3 Colloidal rollers observations and measurements	13
3 Single roller dynamics	15
4 Emergence of collective motion	19
5 Conclusion and perspectives	23
Bibliography	25

Chapter 1

Introduction

These are the experimental results obtained during my master internship in the field of Active Matter for the study and best comprehension of flocks in the laboratory environment. The imposing question of the common features shared by flocks in nature, has driven physicist to build synthetic materials with key parameters that can be controlled at will to study emergent structures and their dynamics, but also to address the beyond issue of how flocks interact with their surroundings. The research done in this subject has been limited and more experimental results are needed to characterize better the phase transitions suffered in collective motion systems. These results could help, eventually, to the better understanding in the physics of flocking and the model of these natural systems.

1.1 Objective

The organized motion perceived in collections of different kind of individuals is an astonishing fact that we frequently observe at any scale: The intriguing issue lies, precisely, in the fact that such dynamics occurs naturally over scales much larger than the size of the single entities, in a great variety of systems. Humans, fish, birds and bacteria organize themselves in herds to move together in any elaborated way, as exemplified in Figure 1.1.



Figure 1.1: Natural flocks. Fish and birds make flocks naturally.

We could assume that any kind of complex behavioral pattern requires complex motives and planning, but certain subjects like bacteria cannot have any complex motives, for they do not have brains. Collective behavior is a common feature of nature and these feats of cooperation sometimes go well beyond swimming in circles.

However, studying these phenomena is considerably complicated (See for example [1], in which collectivities of birds are studied. It is concluded that to analyze the structure, which is the foremost effect of interaction, data on the 3 dimensional positions of individuals in large aggregations must be taken, which is a quantitative problem). So, a model that could be manipulated in the laboratory for the study of collections is needed for a first approach to the problem of flocking. A theory for flocks is needed in a way that we could control parameters in an experimental system and compare its application to natural collective motion.

In the last twenty years, several efforts have been done to motorize soft materials, for making synthetic particles to be used for this purpose, like grains, emulsions, gels and colloids. This motorization makes materials to pass from their passive nature to a self propelled condition. When motorized, and under certain conditions, particles can present patterns formed accordingly to their restraints [2]. Several conventional soft materials have been endowed with the ability to self-propel and some prominent collective dynamical patterns have been recorded, as illustrated in Figure 1.2.

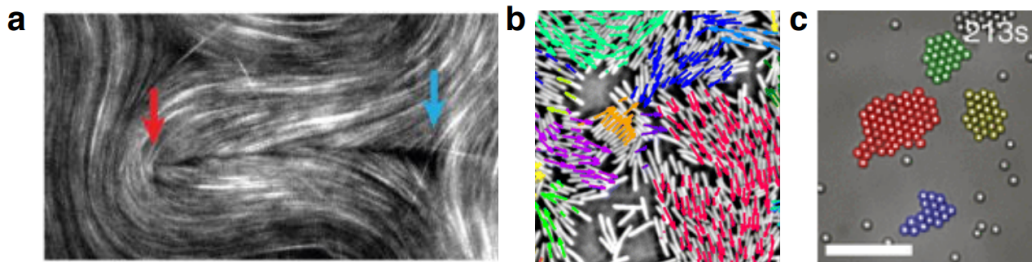


Figure 1.2: Dynamic collective motion in active matter. **a.** Nematic phase of microtubules in movement. Its topological defects merge and nucleate **b.** Cluster of motile bacteria. **c.** Suspension of colloids forming dynamic crystals. Images taken from [3], done to illustrate the variety of collective behaviors in different synthetic active particles

Particularly, between all the collective dynamical patterns, in this report we are interested in flocking, so we are going to focus in polar active materials, that are motile individuals that move in the same direction on average, thereby forming flocks. Our motile units will be called *colloidal rollers*, which are colloids that are made active and they self-propel by the use of the *Quincke rotation mechanism*, as it will be explained deeper in Chapter 2.

We want to study the collective motion of the flocking transition in a model system that was first introduced in [4], using an experimental set up developed by Antoine Bricard [5] and Nicolas Desremaux [6].

1.2 Context and framework

The study of the dynamic collective motion of the synthetic active particles made in the laboratory has revealed a great number of collective behaviors, very different among them. The study of these phenomena does not limit only to flocking and shows different

physical characteristics. This is evident in the different organization of materials (see Figure 1.2), and their study is useful for understanding active matter.

However, we are particularly interested in the emergence of collective directed motion, called *flocking*, in which systems are capable of producing organized and coherent collective motion in a big scale. For the realization of these active materials is first needed to apply a method to propel a great number of particles and then make them interact to align their velocities.

Different strategies have been adopted for this interest and of course the size of the particles, their interaction strategy and the propulsion mechanism changes in all cases. Here we are going to expose some of these methods taken from different research projects.

- **Vibrated polar disks.** The group of Deseigne [7] designed an experiment of self-propelled hard disks. This consists in some circular grains of 4 mm diameter provided by legs of different geometries that are made vibrate vertically in a surface plate, in a uniform way with acceleration relative to gravity. The grains are then self-propelled and they behave as random walkers over the plate.

In this experiment, we can have two control parameters. First, the vibration acceleration Γ can be varied and it is observed that the orientation diffusivity of individual grains increases with Γ . This is because the higher randomization at the collective level lowers the alignment between particles and therefore the collective motion is reduced. Second, the density is also a key parameter. At low density, we observe a gas phase but collective motion is achieved at high density. As density of grains is increased, polar order emerges because the repeated collision between them starts to provoke an alignment in their trajectories. See Figure 1.3.

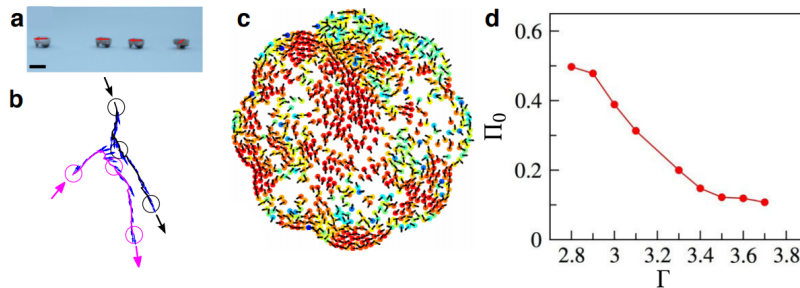


Figure 1.3: Vibrated polar disks. **a** Photograph of grains with legs. **b** Trajectories of vibrated grains during a collision, showing their alignment. **c** Polar flock originated at high density of grains. The perfectly aligned particles are in red and the color scales down until the blue particles (just a few) that are perfectly anti-aligned. **d** The average polarization is the order parameter and it is plotted in function of the acceleration of the plate, which would be the control parameter.

- **Actin filaments.** The group of Schaller [8] made actin filaments active by linking them to molecular motors. Highly concentrated actin filaments are propelled by immobilized molecular motors in a planar geometry when ATP is added to

the system. As a consequence, the protein chain starts to move and different dynamical states emerge depending on the actin filament density. Again, at low density the filaments are seen as random walkers. Above a critical density, filaments self-organize to form coherently moving structures with persistent density modulations such as clusters or bands. Polar clusters emerge at intermediate densities but they are immersed in a gaseous background. Finally, at high density, filaments move collectively with high orientational persistence, polar waves are observed propagating along the same direction.

Characteristic orientational persistence increases with increasing filament density. See Figure 1.4.

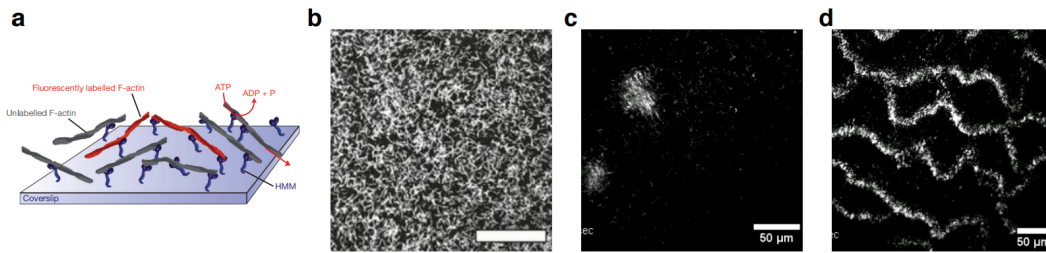


Figure 1.4: Actin filaments. **a** Scheme of experimental set up in which actin filaments are linked to molecular motors. **b** Isotropic gas phase at low density. **c** Polar clusters in a dilute gas at an intermediate density. **d** Polar waves of actin filaments at high density.

- **Self-propelled colloids.** The group of D. Bartolo [4] is focused mainly in the motorization of colloids for the study of flocks, recreating collective movements at big scale. A great amount of polystyrene spheres used as colloids are powered by a DC electric field in a conductive liquid suspension, and are propelled taking advantage of the *Quincke electro-rotation*. This method is the one used in this report and will be explained with detail. The group has used different geometries and obstacles in the microfluidic construction of the set up, to prove their structure, dynamics and interactions with surroundings.

The propulsion mechanism and the interaction between colloids form a gas phase in the low density case and, as the density is increased, assemblies emerge and propagative clusters or bands appear until the high density phase shows a polar liquid and a colloidal flock is created. Another system is the one proposed by Yan group [9] in which Janus particles are made of silica and titanium hemispheres. This particles are powered by an electric oscillating field and the frequency controls the distribution of charges in the hemispheres of the particles. Collective phases are observed too.

See Figure 1.5.

Features shared in the emergence of flocks

From the experiments exposed, we can easily infer a few principles shared by these synthetic flocking phenomena.

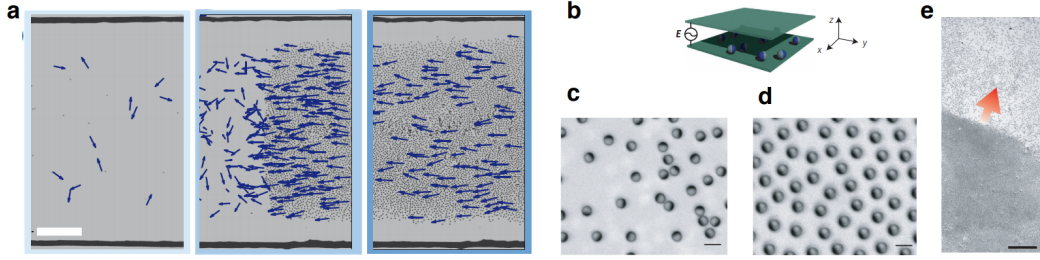


Figure 1.5: Auto-propulsed colloids. **a** Flocking transition in Quincke rollers from gas phase, to the propagative band and finally the polar liquid. **b** Experimental set up for colloids in Yan group [9]. **c** Gas phase. **d** Polar homogeneous phase. **e** Propagative polar band.

First, we can observe **alignment interactions** as a key ingredient for the emergence of flocks. The polar interactions between individuals are necessary for large-scale polar structures as self-propulsion singles out a direction. However, this feature competes with **orientation diffusivity**, because the formation of flocks is impeded by the randomization of the directions of motion at individual level. Finally, a common and important control parameter frequently observed is **density**. As the number of individuals increases, interactions become more frequent and promote the emergence of flocks.

Taking advantage of these features, we could explore the reaching and limitations of the flocking dynamics.

Vicsek model

In 1995, T. Vicsek proposed a model to deduce the origin of directed collective motion [10]. Given that the interaction mechanism in certain systems are diverse and complex, he constructed a microscopic model of physical interactions that should be enough to explain the emergence of order at big scale. He basically presented the consideration of describing flocks as active ferromagnets, so it is a Heisenberg-like model in which pointwise particles at density ρ are moving off-lattice at velocity v_0

The idea is basically that at each time step a given particle with a certain constant absolute velocity v_0 , will assume the average direction of motion of the particles in its neighborhood in a circular area of radius R , with some random perturbation added. This happens for every particle at each instant of time, giving the physical idea that the particles interact with each other in time, aligning between them with a certain noise that gives the random component to the orientations.

Translated into equations, the position \mathbf{r}_i and angular orientation θ_i of particle i will be, correspondingly,

$$\mathbf{r}_i(t + \Delta t) = \mathbf{r}_i(t) + v_0 \hat{\mathbf{v}}_i(t) \Delta t \quad (1.1)$$

Where $\hat{\mathbf{v}}_i$ is the unitary vector pointing in the orientation of the particle. In the model, the interactions do not alter the speed but they act as torques that change

particle orientation, so:

$$\theta_i(t + \Delta t) = \langle \theta_j(t) \rangle + \eta \xi_i(t) \quad (1.2)$$

Where j are the particles in the neighborhood of a circle of radius R , $\langle \theta_j(t) \rangle$ is the average orientation of those particles, ξ_i is a random variable with zero mean and unit variance and η is a noise strength.

The Vicsek model is an analog of the ferromagnetic model, except in the fact that the ferromagnetic model is an equilibrium model in which spins are aligning. Instead, in the Vicsek model the direction of motion is the variable that aligns.

The evolution of this model is given by the control parameters that are, in this case, the constant velocity v_0 of the particles, the density ρ and the noise force η . If the density is increased or the noise is reduced, the flocking transition and the emergence of collective motion can be found in Vicsek model. The order parameter, in analogy with the magnetization in the ferromagnetic model, will be the polarization of the system $\Pi = \langle \theta_i(t) \rangle$, which will be equal to 1 in the ordered phase and equal to zero in absolute disorder of orientations.

We will be passing from a gas phase to a critical point in which propagative polar bands appear in a disordered background (coexistence phase), until finding a polar phase with orientations aligned. We will have a first order phase transition due to the emergence of the coexistence phase, but this is surprising because this situation does not exist in ferromagnets. Also, the polar liquid phase shows long-range order, which would be impossible in 2 dimensions for equilibrium systems. However, these features have been displayed in a variety of models for flocking, showing the validity of Vicsek model.

Flocking transition in Vicsek model

The Vicsek model has three independent control parameters: The density ρ , the particle velocity v_0 and the noise strength η .

Alexandre Morin [11] has conducted in his thesis some simulations for the vibrated grain experiments exposed before, using the Vicsek model and focusing on the role of the noise strength η because it plays a role similar to temperature in equilibrium systems. The order parameter in these simulations is the polarization, that allows to characterize the transition between order and disorder.

As expected, ordering occurs upon decreasing noise strength. At high η , particles behave as a homogeneous and isotropic gas. When arriving to a threshold η^* , the polarization increases sharply (the flocking transition is discontinuous, so of first order nature), the rotational symmetry is spontaneously broken and a dense flock emerge coexisting with a gas phase, just as in the grains experiment. However, the flock is a stationary structure that behaves as a wave because particles are exchanged between the gas and the flock. Finally, at low η , there is just a flock homogeneous in density and orientational order. This polar liquid is the analogy to the active ferromagnet.

Toner and Tu model

From a theoretical point of view, the Vicsek model and its reliability surprises because of two reasons: the coexistence phase that it prevents and the existence of a polar liquid phase in itself.

The fact that an heterogeneous state can be observed in flocking systems is intriguing because this phenomenon is not possible in ferromagnetic systems. And this is not less curious than the fact that in polar liquids we observe long-range order at equilibrium but that this would be impossible in two dimensions, as prevented by the Mermin-Wagner theorem.

Because of these observations, we can suppose therefore that the explanation is found in the microscopic mechanisms of the system. As a consequence, Toner and Tu [12] proposed a complementary perspective to flocking based on an hydrodynamic theory. They built an analogous of Navier-Stokes equations for flocks, regarding them as spontaneous flowing liquids. It is a non equilibrium model and their equations govern the evolution of the density $\rho(\mathbf{r}, t)$ and velocity $\mathbf{v}(\mathbf{r}, t)$ fields for large time and length scales.

In its minimal version (for a rigorous derivation see [4]), we can write Toner and Tu equation as

$$\partial_t \mathbf{v} + \lambda(\mathbf{v} \cdot \nabla) \mathbf{v} = -\sigma \nabla \rho + D \Delta \mathbf{v} + (a_2 - a_4 |\mathbf{v}|^2) \mathbf{v} \quad (1.3)$$

Where the red part corresponds to the equivalent of the Navier-Stokes equation and the blue part is the contribution of the Ginzburg-Landau functional. The term $-\sigma \nabla \rho$ represents a pressure term that suppresses density fluctuations and $D \Delta \mathbf{v}$ is a viscous contribution.

In the model, we have the usual advective and convective contributions of hydrodynamics, but we need a term that governs the existence of collective motion. For a collective moving state with velocity v_0 to be favored, this term must change sign from positive to negative at $|\mathbf{v}| = v_0$, so this is why we get a Landau force given by $(a_2 - a_4 |\mathbf{v}|^2) \mathbf{v}$, in which a_2 and a_4 may depend on ρ and be positive.

This contribution accounts at the hydrodynamic level for microscopic alignment interactions and an homogeneous polar liquid with arbitrary small velocity can form.

The coexistence of flocks and gas in Vicsek model suggest that solutions for Toner and Tu equation do exist.

Toner and Tu evidenced that polar liquids exhibit true long-range order in dimension 2 unlike equilibrium systems. This is obtained going beyond linear approximations around the polar liquid state by taking fluctuations and non-linear contributions into account. Also, they showed that the polar liquid displays giant density fluctuations due to sound modes.

We can say, then, that a physics of flocking does exists and that its theory needs just experimental corroboration. Regarding the characterization of the polar liquid phase, many efforts have been devoted to the measurements of the density fluctuations but the accuracy and confidence in the results are somehow limited.

1.3 Research Plan

In active matter systems, as it has been shown, the self propelled particles interacting in groups derive in emergence of flocks. This directed collective motion is strongly dependant in the density of the polar active particles, and present normally a phase transition between the gas phase at low density and the polar liquid at high density.

Taking this into consideration, I will follow the strategy proposed by D. Bartolo and his group [4] for the auto-propulsion of colloids, using particles of different sizes and testing the experimental set up for making colloids roll in a circular geometry, as it will be explained later. The experimental results will be used for the phase transition analysis.

I will start by exposing the methods used for the study of these particles, then I will characterize their singular behavior to arrive finally at a conclusion on their collective dynamics of flocking. Meaningful experimental results will be shown for clarity.

Chapter 2

Materials and Methods

In the field of soft matter physics a great variety of materials, from grains to gels, have been motorized for their study, changing their passive nature to turn into self-propelled particles. In particular interest, there is the case of colloidal rollers, which are colloids made active by the use of the Quincke rotation mechanism. I first describe how Quincke rotation works, as it was first introduced in [4] and then I present the experimental set-up of my work, originally developed by [5, 6]

2.1 Colloidal rollers motorization principles

The objective of this section is to explain how to motorize a certain population of colloidal particles. The colloids are made active by the use of the Quincke rotation mechanism. This motorization principle is based on the effect of an electro-hydrodynamic instability, known as the Quincke effect [13].

When a spherical insulating colloid particle is immersed in a conducting liquid and a constant electric field \mathbf{E}_0 is applied to it, the conductive charges accumulate in the surface of the particle and a dipolar distribution appears between the charges due to the charge transport within the fluid. The dipole \mathbf{P} points in the exact opposite direction of the electric field, as it can be seen in Figure 2.1a, so the colloid is immobile.

This configuration is stable for certain values of \mathbf{E}_0 , because the fluctuations are overdamped for sufficiently low electric field. However, over a certain critical value of electric field \mathbf{E}_Q , called the Quincke threshold and which depends on the material properties of the fluid and the colloid, the distribution of the surface charges breaks spontaneously the rotation symmetry and the system becomes unstable. The distribution is still dipolar, but the direction of \mathbf{P} forms an angle with the electric field and the fluctuations in the orientation lead to an electric torque $\mathbf{P} \times \mathbf{E}_0$, that will favor rotation, as seen in Figure 2.1b.

Above the Quincke threshold, the sphere rotates at a constant speed Ω that increases with the applied electric field \mathbf{E}_0 . It is important to notice that the direction of rotation occurs clockwise or counter-clockwise with *equal probability*. The dynamic stationary state is reached when the electrostatic pair is balanced by the viscous friction and can be converted into translational velocity if the colloid is simply deposited over a plane surface, as seen in Figure 2.1c. This colloid is then called *Quincke roller*.

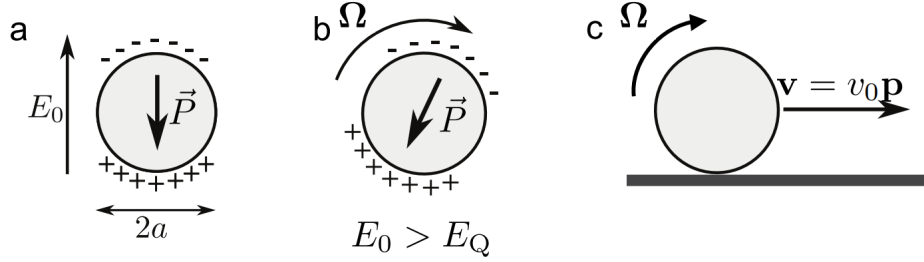


Figure 2.1: Quincke electro-rotation. (a) The dipole \mathbf{P} generated by the surface charges is oriented in the exact opposite direction of the electric field E_0 , in a colloid of radius a . (b) For electric fields bigger than the Quincke threshold E_Q the colloid starts to roll with a constant rotation speed Ω . (c) Transformation of rotation movement into translation when the colloid rests over a plane surface. The direction \hat{p} is random and the speed v_0 is constant.

We can say therefore that the Quincke mechanism corresponds to a spontaneous breaking of symmetry, so all the orientations of the movement are identically distributed on the surface plane. The viscous friction of the liquid tends to suppress rotation, so the competition between the electric torque and the viscous friction depends on the field amplitude, making the fluctuations overdamped below the Quincke threshold and favoring the stability of the system in this regime. Thereafter, it breaks rotation symmetry over the Quincke threshold, making the system unstable. In this regime the rotor reaches a new steady state with a constant rotation speed given by (see [14] for details):

$$\Omega \propto \sqrt{\left(\frac{E_0}{E_Q}\right)^2 - 1} \quad (2.1)$$

And the dynamics of an individual particle is given by:

$$\mathbf{v} = v_0 \mathbf{p} \quad (2.2)$$

With \mathbf{p} the polarization of the particle and $v_0 = a\Omega$ the constant speed at which colloids move, where $a \sim 5\mu\text{m}$ is the radius of the colloid.

Given that there is no privileged direction in Quincke mechanism, the propulsion mechanism doesn't allow the modification of the orientations once the rollers are moving. Also, the surface in which rollers move is not ideally planar, thermal fluctuations perturb the orientations and then the Quincke rollers behave as random walkers, like Brownian particles with speed v_0 and orientation diffusivity D , so the motion equations of a roller i are:

$$\dot{\mathbf{r}}_i = v_0 \hat{\mathbf{v}}_i \quad (2.3)$$

$$\dot{\theta}_i = \sqrt{2D} \xi_i \quad (2.4)$$

Where ξ_i is a white gaussian noise with zero mean and unit variance, $\mathbf{r}_i(t)$ is the position of the colloid and $\hat{\mathbf{v}}_i(t) = (\cos \theta_i(t), \sin \theta_i(t))$ the direction of motion.

2.2 Motorizing, Handling & Observing colloidal particles

We use the Quincke mechanism to induce rotation in polystyrene colloids of two different radius, $a = 5\mu m$ and $a = 10\mu m$, centering mainly in the bigger ones, as we will see later.

The colloids are insulating spheres suspended firstly in water, so it is necessary to clean them before and transfer them into a conducting liquid with an adequate viscosity to be able to induce rotation through Quincke motorization. The conducting liquid is a mixture of dioctyl sulfosuccinate sodium salt (AOT) and hexadecane. The hexadecane gives the liquid viscosity and its conductivity is regulated by the amount of salt dissolved. Typically, I used a solution of 0.12 mol/l of AOT in the hexadecane.

For cleaning the colloids, they are first dispersed in the suspension by ultrasound, and then centrifuged and extracted with a pipette, proceeding next to inject them in the mixture of AOT+Hexadecane and repeating this procedure a dozen times, to make sure to remove all the water in the solution. If the water is not removed completely, it can modify the surface charges of the colloids and affect their displacement.

We can modify and control the density at which colloids are going to be studied, and they can be injected in a microfluidic chamber at different concentrations for the experimentation. The microfluidic chamber, as the one schematized in Figure 2.2, is the experimental device useful for the study of a great number of colloids (of the order of millions), and is constructed in the following way:

- **Patterning.** We have two glass slides with their inner part covered with a layer of indium tin oxide (ITO). The ITO layer makes them electrically conducting. The inner part of the bottom glass slide is covered with a resin, which is made with an insulating material. Then, certain parts of this resin are removed with UV lithography to create patterns in which the colloids are going to roll. For the case of my experiment, I used circular chambers designed in a mask that was used for the removal of the resin, as seen in Figure 2.3. The chambers are of 1.5 mm radius.
- **Drilling.** In the upper glass slide, two holes are drilled close to the borders, through which microfluidic connections are going to be made.
- **Sticking.** The two glass slides are stucked together using a hollow double-sided tape of $25\mu m$ height. This creates a pool between both glass slides, in which colloids are going to be injected and then sediment to make contact with the bottom slide planar surface to roll.
- **Microfluidic connections.** Two tubes are connected to each hole of the upper glass slide using again a double-sided tape. From one side, colloids are injected in the device and they will be able to go out from the other side.
- **Electric connections.** The two glass slides are connected through electric wires to a power supply, to work as electrodes when applying a DC electric field in the \hat{z} direction.

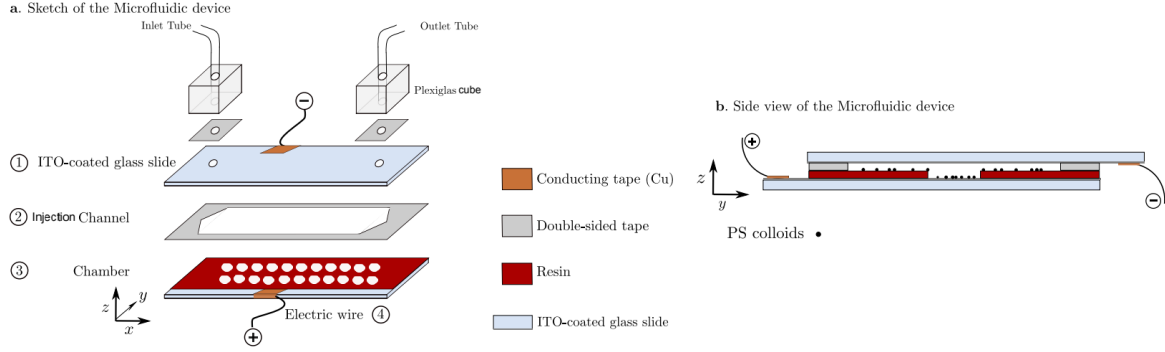


Figure 2.2: Microfluidic device. (a) Schematic assembly of the experimental device. (b) Side view of the device. The colloids fall in a chamber and roll only when turning on the power supply and if they are not in contact with the insulating resin. The double-sided tape has a height of $25 \mu\text{m}$, while the colloids have a height of only $5 \mu\text{m}$ or $10 \mu\text{m}$, depending on the experiment done.

The colloids suspended in the conducting liquid are injected inside the device with the use of a syringe and then they sediment. It is important to notice that even if the injection is done homogeneously within the pool, when turning on the electric field just the ones within the chambers of removed insulating resin will roll.

The great advantage of using this kind of microfluidic device lies in the possibility of controlling the flow of a big amount of colloids with high precision and in the versatility for patterning in different ways the chambers for the study of flocks.

The observation of the colloids in the chambers is done very easily through a microscope and a system for registration of images. We use a microscope Nikon AZ100 Multizoom and focus in the inside of one of the chambers, as seen in Figure 2.3. The colloids can be seen clearly within the chamber using the proper zoom and focus.

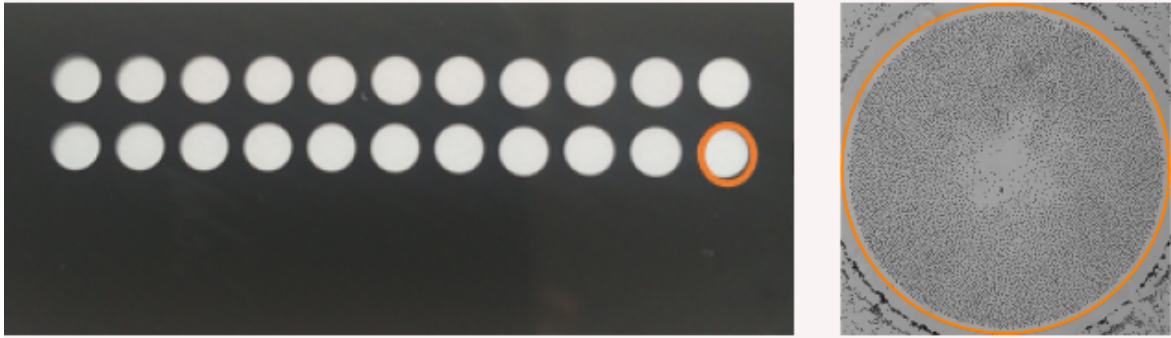


Figure 2.3: Experimental image. Left: Mask used for the patterning of circular chambers in the device. Each chamber has a radius of 1.5 mm . Right: The colloids suspended in the conducting liquid are injected in the device and observed within a chamber (orange circle drawn in the picture) through a microscope. Images are recorded with a camera.

2.3 Colloidal rollers observations and measurements

Since our objective is that of observing flocks and describe the transition between low density and high density colloid populations, it is important to take into account the instantaneous positions and velocities of millions of particles at the same time. This is done in a series of steps.

- **Observation.** Colloids are observed through the microscope with an x3 objective and the experimental videos are registered with a CMOS camera at high frequency (190 Hz). The images have a size of 2000x2000 pixels coded in 8-bit and they are saved on hard disks of large storage capacity. We are interested in the stationary state of the system, so images are recorded measuring the current between the electrodes and waiting 5 minutes after the injection each time. The temperature of the system is kept fixed at 23 °C. For the experimental process, we focus with the microscope in one of the chambers, the colloids are injected each time at different densities ρ_0 and assumed to be distributed uniformly over all the surface. After waiting for sedimentation over the bottom electrode, the electric field is turned on and the colloids inside the chamber start to roll. We wait for the stationary state, the current and the temperature are measured each time, and images are recorded for about 5-6 seconds for each density. This is done for different densities and different electric fields, to be able to construct the phase diagram later. The images observed and recorded are as those shown in Figure 2.4a. and Figure 2.4b.
- **Detection.** For the analysis of the dynamics of particles, we need first to obtain the positions of all the rollers in every image. For doing this detection, I used an algorithm implemented by Peter Lu [15]. The code was modified by Alexandre Morin [11] in his thesis to subtract the background of the images before the detection and avoid impurities to be detected. The fineness in the code for the detection of a great quantity of colloids is qualitatively shown in Figure 2.4c. Therefore, the calculation of the density of colloids ρ_0 in each experiment is done with great reliability after the detection of all particles in each image, considering that $\rho_0 = \frac{N_{colloids}}{A_{circle}}$, where A_{circle} is the total area of the chamber. The density ρ_0 for each experiment is given as an average of all the images analyzed and corresponds to a percentage of the chamber area covered by colloids. To give an order idea, a density of $\rho_0 = 5\%$ corresponds to an order of 10^4 colloids of 5 μm radius.
- **Tracking.** After detection, it is then necessary to track the trajectories of each particle, to construct the field of velocities. For the tracking, it is used an algorithm written in Matlab by J.C. Crooker and D.G. Grier [16]. The algorithm labels each particle and follows them in time, considering each image after the previous one. It is necessary to consider in the code that the maximal displacement of particles should not be bigger than the distance between particles. For making the code work properly, the images are taken with the high frequency of 190 Hz. The code permits then to take averages on time for the particles and measure the value of the average speed v_0 of the Quincke rollers. The tracking

images obtained are like the one shown in Figure 2.4d. With the information provided by the tracking of the rollers is possible to generate histograms of velocity and fields.

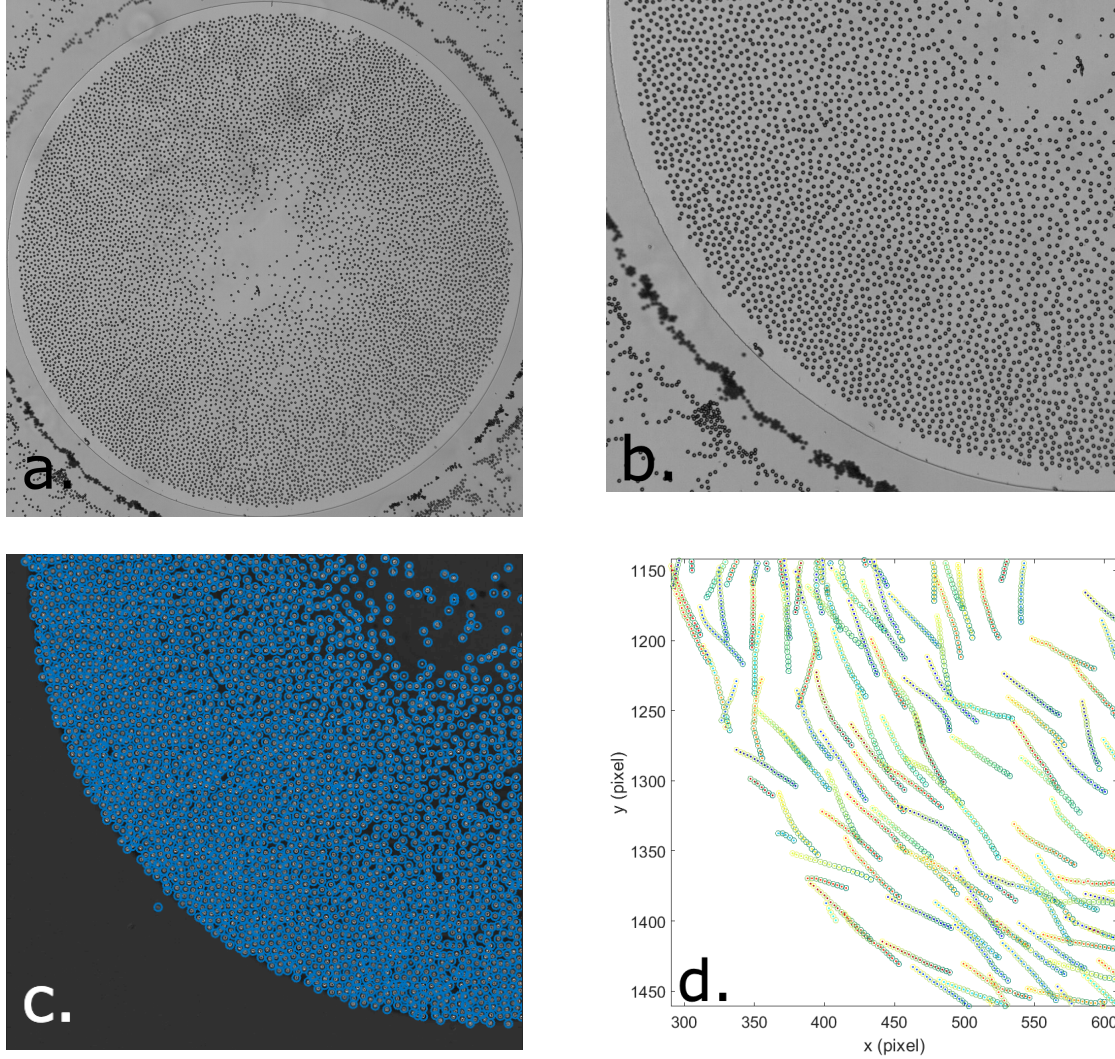


Figure 2.4: Analysis process of experimental images. (a.) Observation of colloids ($\sim 20,000$) through an x3 objective microscope inside a circular chamber of 3 mm diameter. (b.) Zoom to the inferior left quarter of the image. (c.) Detection process of the image. Every blue circle corresponds to the detection of one particle. (d.) Reconstruction of the rollers trajectories in 20 images. Done for every pixel of the images recorded, considering the maximum displacement of particles for each image.

After describing the process of the electro-hydrodynamics instability of Quincke mechanism to motorize colloids, their behavior as active brownian particles, the experimental set-up used for their study at circular chambers for different densities and sizes, the detection and tracking process for saved images, and the versatility of this experimental system, it is now possible to study the flocking behavior of these particles.

Chapter 3

Single roller dynamics

For studying the dynamical transition between disorder and order in a Quincke colloidal system, we start primarily by characterizing the individual dynamics of the rollers. For doing this, we work first with a diluted population of colloids, in a low surface density order ($\rho_0 \sim 0.2\%$ for colloids of $5\text{ }\mu\text{m}$ radius and $\rho_0 \sim 0.1\%$ for colloids of $10\text{ }\mu\text{m}$ radius). The density is fixed while the colloids are rolling inside a chamber of 3 mm diameter.

For the first experiment, we keep fixed the potential difference between the electrodes of the chamber at 120 V (at which colloids are seen to roll around all the chamber) and record images for the $10\text{ }\mu\text{m}$ radius colloids. In the top left image of Figure 3.1 we can observe one of my experimental results of the persistent paths made by these rollers in a diluted surface density phase inside of one of the chambers of 3 mm diameter. These paths were traced with *ImageJ*, using superimposed snapshots of successive images of the experiment. From now on, the low density regime is called *Gas phase* for its disordered quality, as it can be seen directly in the image.

In the top right image of the same figure, a zoom is made to the trajectories, observing qualitatively that the colloids have a similar spacing between images along the trajectories, so we could infer that they move at constant speed in various directions, following no apparent order. This image shows that rollers do not move along straight lines and instead they diffuse orientationally. This could be due to surface heterogeneities, considering that the surface is not ideally plane, or to brownian diffusion of surface charges involved in the Quincke mechanism [3] (However, Morin [11] quantifies this orientation diffusivity by measuring the velocity orientation correlations of the colloids. He observed that the typical rate of the decorrelation considering ion clouds of size $100 - 10\text{ nm}$ is of the same order of magnitude as the one that would yield to consider Brownian diffusion of the surface charges involved in the Quincke mechanism).

After tracking the trajectories of the particles, we can represent the probability density $\mathcal{P}(v_x, v_y)$ of the individual velocities of the colloids in the system and make an histogram of the rollers velocities, decomposing the velocity on the v_x and v_y components.

We observe in the down image of Figure 3.1, that the histogram for the gas phase for the $10\text{ }\mu\text{m}$ radius colloids is a circle in which the count of particles has a peak in the distribution at a radius distance of $v_0 = 1.1\text{ mm/s}$. This speed correspond perfectly with the estimation of Quincke theory of $v_0 \simeq 1\text{ mm/s}$ (see [3, 11]).

We can see a uniform yellow circle in the image, in which definitely no direction

is privileged. This is an important result, showing immediately one of the effects of Quincke motorization in the gas phase: The axisymmetric form of the distribution shows that it is *isotropic*, confirming the random choice of direction taken by each particle at an average same constant velocity v_0 , as the Quincke motorization predicted. The fluctuations around this velocity are negligible.

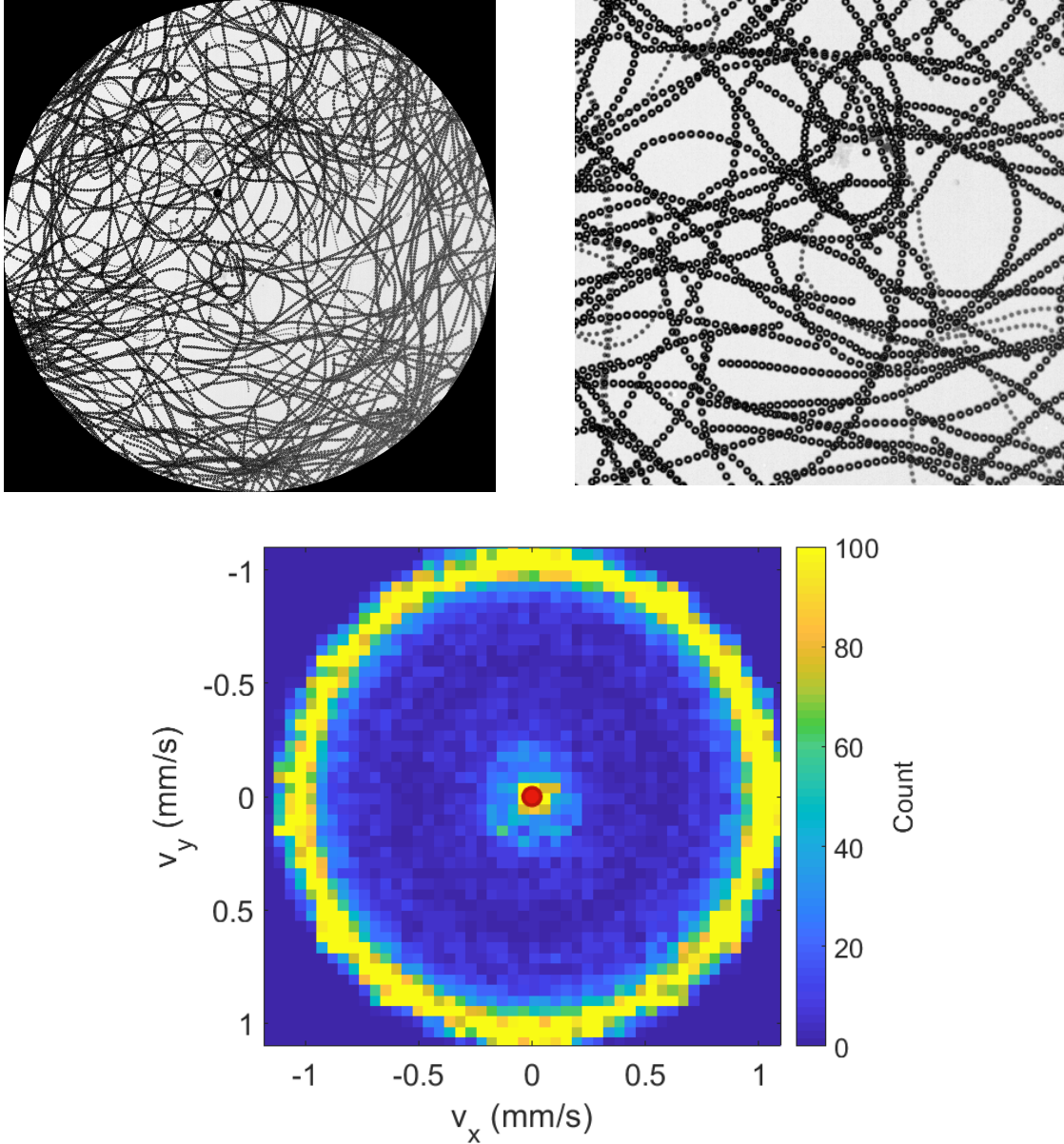


Figure 3.1: Gas phase. Top left: Experimental image of the trajectories of low density colloids rolling in a circular chamber (120 V). Top right: Zoom to the trajectories inside the chamber. Down: Histogram of the rollers velocities. The red dot indicates the center.

Even if in the experiment illustrated we can see also a peak around the zero velocity (the red dot that indicates the center), this is due to the fact that for the $10\ \mu\text{m}$ radius colloids experiments, there are a lot of them sticking in the chamber at different

positions, producing a tracking of a considerably large amount of particles fixed and immovable. These bigger colloids are considerably harder to handle immersed in the conductive AOT+Hexadecane liquid, considering that they have a larger surface area than the $5\ \mu\text{m}$ radius colloids which move more smoothly, as it can be seen in Chardac thesis [17] for the same characterization results in these smaller colloids.

For the next experiment, we consider now the case of the gas phase for the $5\ \mu\text{m}$ radius colloids. In this case, we keep fixed the low surface density of colloids in the chamber but we change the potential difference between the electrodes, varying it from 60 V to 180 V. In Figure 3.2 we can see that effectively the average value of the speed of particles increases with the potential difference and, consequently, with the electric field $E_0 = \frac{V}{d}$, where $d = 25\ \mu\text{m}$ is the separation between electrodes, and V is the potential difference.

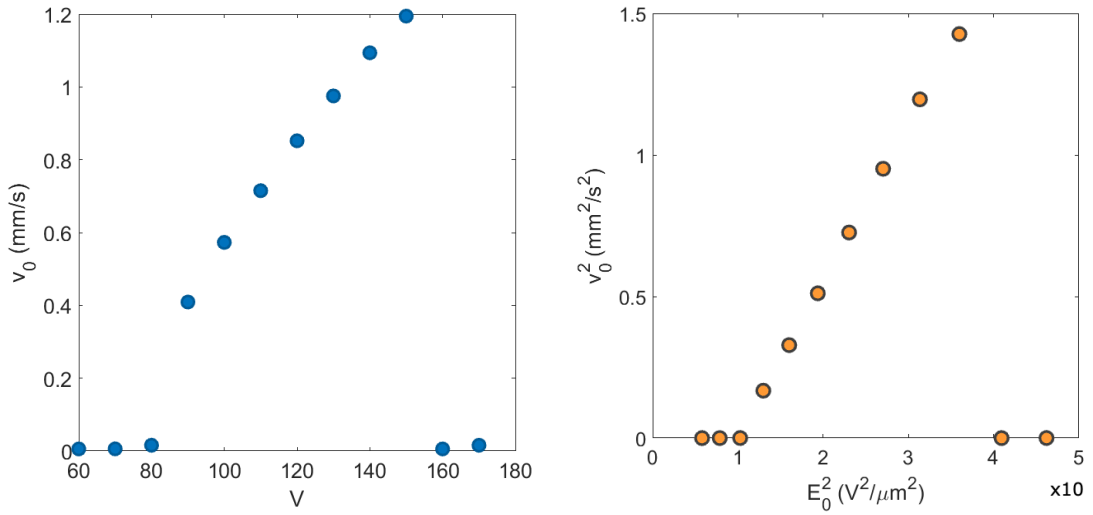


Figure 3.2: Variation of velocity with the electric field E_0 . Left: The roller speed v_0 increases with the potential difference V and, consequently, with E_0 . Before the Quincke threshold, the speed is zero, and comes back to zero from the Quincke freezing point at 160 V. Right: v_0^2 increases linearly with E_0^2 as predicted by Quincke theory.

For low values of V , as seen in the left side of Figure 3.2, the rollers speed is zero. In this regime we have the dipole of the roller pointing in the opposite direction of the electric field, because fluctuations are overdamped by the viscous friction of the liquid, as predicted by the theory, and the colloids don't move. At the Quincke threshold, occurring approximately at 90 V ($E_Q = 3.6\ \text{V}/\mu\text{m}$) for an AOT+Hexadecane solution of 0.12 mol/l, the colloids start to roll spontaneously, and the rotor speed increases with the applied electric field E_0 .

The right plot of Figure 3.2, shows that v_0^2 varies linearly with E_0^2 , as predicted by the theory in Equation 2.1. However, we can see that from 160 V, the colloids *freeze* again and stop moving. Experimentally, at this point colloids are just seen vibrating in their fixed positions, so the speed v_0 comes back to zero in this regime. The value of this electric field is known as the *Quincke freezing point*., and the causes of the phenomena

of freezing particles in higher fields that was observed during experimentation are still unknown and are under research.

The Quincke threshold is equal to [4]:

$$E_Q = \sqrt{\frac{8}{3} \eta \frac{\sigma_l}{\epsilon_l \epsilon_p}} \quad (3.1)$$

Where η is the fluid viscosity, σ_l is the fluid conductivity, and ϵ_l and ϵ_p are the dielectric constants of the liquid and the colloid respectively. This shows that the Quincke threshold depends on the liquid and colloid properties, and that from our results we can also characterize the materials used.

The figures shown in this chapter demonstrate that our rollers, tested in gas phase for characterizing their dynamics, are following Quincke mechanism, and we can center particularly in the 10 μm radius rollers in which we are now interested in.

Chapter 4

Emergence of collective motion

After characterizing the individual dynamics of Quincke rollers focusing on the low density regime or *gas phase*, it is time to move our attention to the high density or *Polar liquid phase*. Using the same 3 mm diameter chamber, we can now control the injection of colloids to progressively, having a larger surface densities inside it. In this case, we leave the potential difference fixed to a value of 120 V in which we are sure colloids are rolling freely, and we modify the density of the colloids suspended in the conductive liquid using a high precision syringe in the experimental set up.

Eventually, around a value of $\rho_0 = 0.4\%$ for the case of the $10\ \mu\text{m}$ radius colloids and of $\rho_0 = 0.3\%$ for the $5\ \mu\text{m}$ radius case, we are able to distinguish a transition between the gas phase and the polar liquid phase, in which colloids seem to self-organize in an orientational way, generating a *vortex* that turns around the circular chamber, with all the colloids rolling in the same direction, forming circular trajectories like rings around the center of the chamber.

This phenomena can be seen in Figure 4.1(a.), where we can see an experimental picture for the $10\ \mu\text{m}$ radius colloids case, having the vortex of the polar liquid on the right side in contrast with the disordered gas phase on the left. In this figure, the pictures are presented as a function of density ρ_0 . As density increases, we approach to the polar liquid phase, with a self-organized behaviour of the colloids. Instead, as it decreases and we arrive to the low surface density of rollers, we will be in the gas phase.

The collective motion shown in the self-organized dynamics of the vortex in the polar liquid, shows the existence of *flocking* in synthetic colloids. When the colloid surface density is incremented, the rollers are constricted to interact between them with a higher probability, so the flocking transition comes out from this interaction.

In Figure 4.1(b.) we can see the field of instantaneous velocities zoomed in the left bottom quarter of the upper images. This lets us see the order present in the polar liquid phase and the direction of the velocity vectors followed by this experimental case. The comparison with the random direction of the velocity field in the gas phase is qualitatively evident from this image.

Finally, the density field for both cases can be calculated after the detection of particles in the images recorded, and it is observed in Figure 4.1(c.). The yellow zones of the density field $\langle\rho(\mathbf{r}, t)\rangle_t$ correspond to the largest concentration of colloids in the experiment and the blue ones to the lowest.

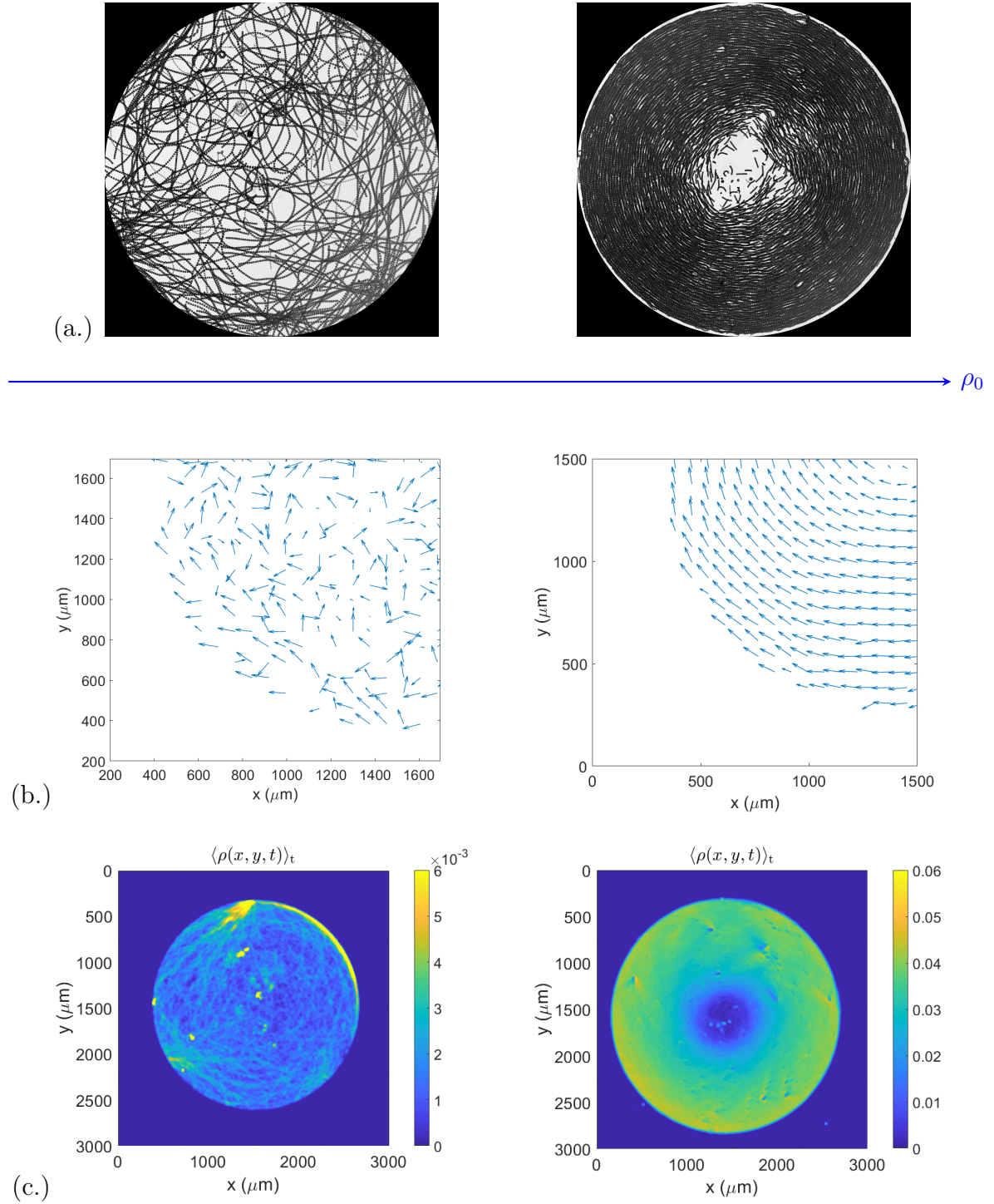


Figure 4.1: Gas phase vs Collective behaviour in polar liquid. (a.) Experimental images in function of density ρ_0 . (b.) Velocity field obtained after tracking. Each blue arrow corresponds to a velocity vector in that point of space. (c.) Density field obtained after detection.

Therefore, we can see that in the case of the polar liquid, the concentration of colloids goes from maximum near to the walls of the chamber to gradually reduce

towards the center. Instead, in the gas phase, the density is considered homogeneous over all the chamber, except by some impurities and stuck colloids in certain zones of the chamber. The counting of colloids is obviously less in the case of the diluted gas phase.

On the other hand, I also obtained plots as the ones shown in Figure 4.2. Given the symmetry of the system, we can characterize the transition from gas phase to polar liquid phase using circular geometry and decomposing velocity in its radial v_r and angular v_θ components. We can plot v_θ as a function of ρ_0 (like in the bottom plot for the case of the 10 μm radius colloids), or the average polarization projected on the orthoradial axis $\langle \Pi_\theta(\mathbf{r}, t) \rangle_{t,\mathbf{r}}$ as a function of ρ_0 , to get the value of the order parameter.

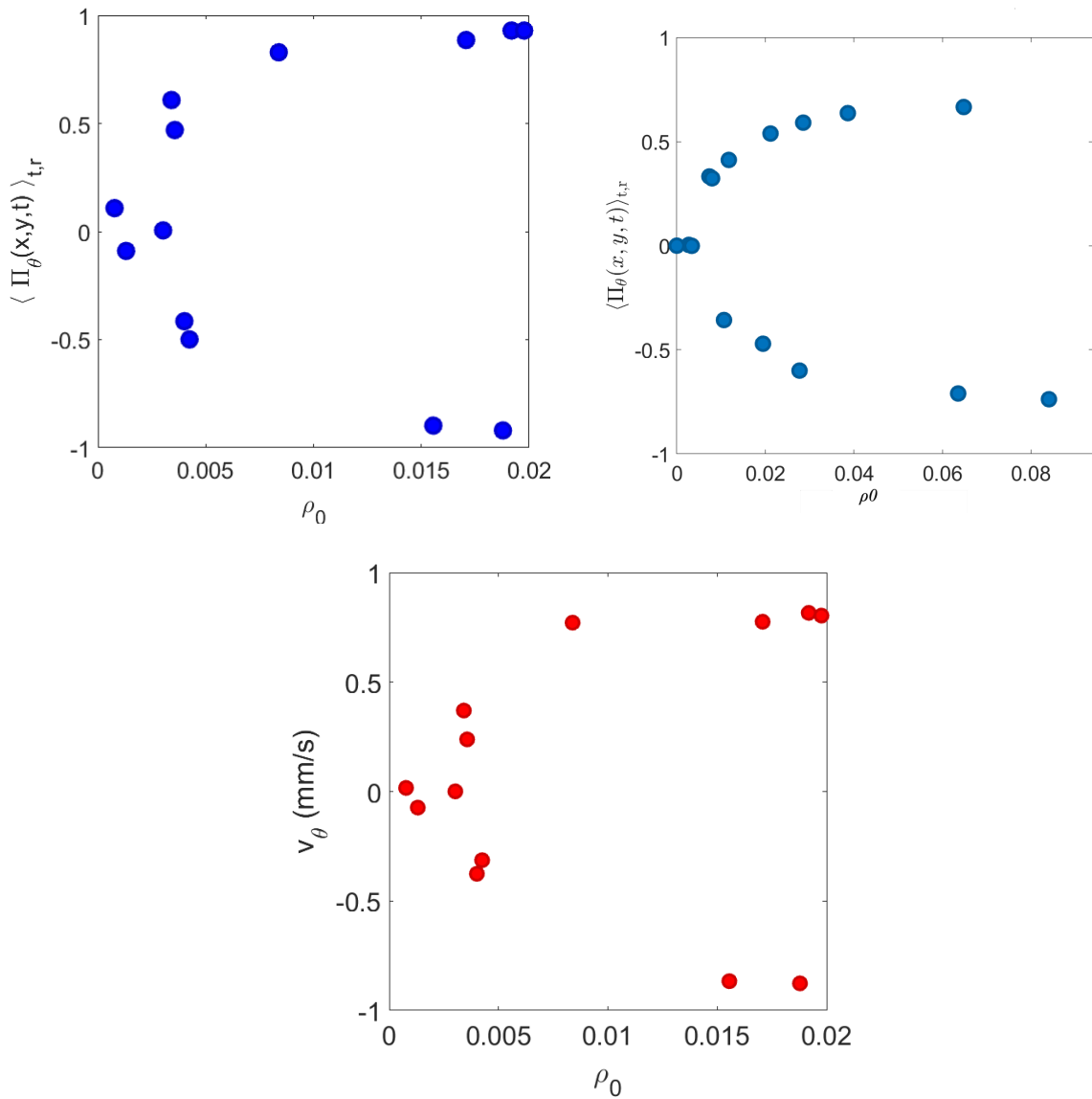


Figure 4.2: Order parameter vs Area fraction of colloids Top left: Average polarization for the 10 μm radius case. The transition occurs at $\rho_c \simeq 0.004$ in this case. Top right: Average polarization for the 5 μm radius case. The transition occurs at $\rho_c \simeq 0.003$ in this case. Down: v_θ vs ρ_0 for the 10 μm case.

We use the average polarization $\langle \Pi_\theta(\mathbf{r}, t) \rangle_{t,\mathbf{r}} = \frac{\langle v_\theta \rangle}{v_0}$ as the order parameter in analogy to the magnetization for a spin system. The top images of Figure 4.2 represent the values of the order parameter obtained experimentally for two sizes of colloids as a function of the area fraction of the particles. We can see then the bifurcation transition for the colloids of $10 \mu m$ radius and for the $5 \mu m$ radius, respectively.

When the order parameter is zero, it means that there is no collective movement at great scale, which is the case for the gas phase in a dilute concentration of colloids. As the density is increased, the system arrives to a critical value ρ_c from which it suddenly breaks rotational symmetry and $\langle \Pi_\theta(\mathbf{r}, t) \rangle_{t,\mathbf{r}}$ becomes not-zero, approaching in a concave and smooth way to 1, the maximum value. This occurs because the colloids polarize spontaneously in a sense or in the other along the orthoradial axis. In this case, we are observing the polar liquid phase, with the colloids forming a flock that is rotating.

For the $10 \mu m$ radius colloids case, the transition occurs at $\rho_c \simeq 0.004$. In a slightly different situation, for the $5 \mu m$ radius colloids case, the transition occurs at $\rho_c \simeq 0.003$ as it is also shown by Chardac [17], and the order parameter value grows slower, due to the fact that the colloids are smaller, the probability of encounters between them is lower and more of them are required to produce effective interactions.

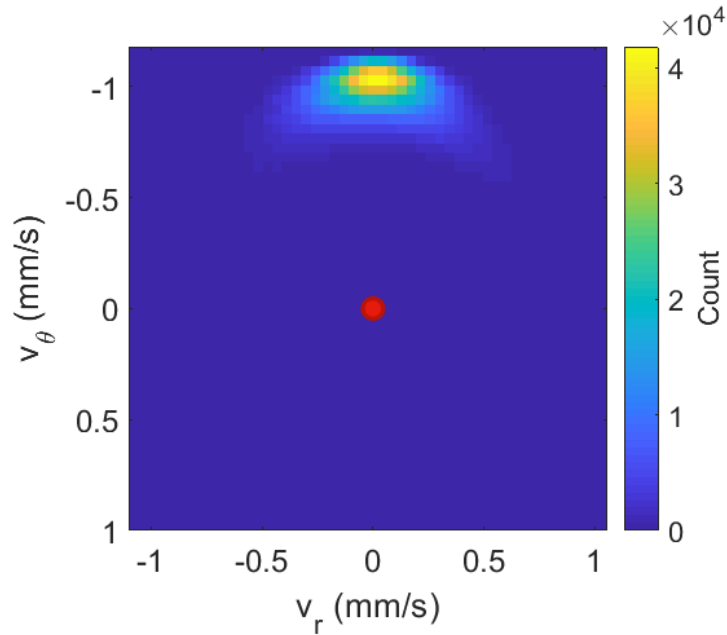


Figure 4.3: Histogram of rollers velocities for a polar liquid. The velocities are mostly oriented in the orthoradial direction.

Going back to observe the trajectories followed in a polar liquid (Figure 4.1a.), we can see that all the particles roll in the same sense. We can plot the histogram of these rollers velocities and confirm it by showing that in this case there is a privileged orientation chosen. As presented in Figure 4.3, the great majority of particles in the chamber have on average their velocity aligned with the orthoradial axis. In the formation of the vortex, the center of the chamber is almost empty and closer to a gas phase, and the system cannot separate in phases [18].

Chapter 5

Conclusion and perspectives

We have been able to carry out an experimental study thanks to a model system that is used to characterize the emergence of collective motion in polar liquids, focusing on the comparison of different values in size of particles, density and electric field used in previous research papers, familiarizing with the experimental model and testing the robustness of the theory for these variations.

This model made possible to observe a large number of self-propelled particles on the evolution of collective motion with the variation of density. The phase diagram that we have established with the colloid density as parameter, reveals the presence of the two main states of the system, separated by phase transitions. In particular, we have highlighted that the transition occurs at a slightly higher density for the bigger colloids and that the order parameter value, in comparison with the tinier ones, grows faster when the system is already in the polar liquid phase, which is mainly due to the bigger size of the particles and the higher probability of encounters between them, making more effective interactions for the alignment of velocities.

In addition, I want to mention that the appearance of the Quincke freezing point for high electric fields as mentioned in 3 have not been discussed at all. This is a phenomena that should be studied in further work.

It would be particularly interesting to observe and characterize the emergence of flocking in different geometries and combining different size of particles, to observe the effects in the variation of more variables.

Bibliography

- [1] C. R. e. a. Ballerini M., Cabibbo N., *Interaction ruling animal collective behavior depends on topological rather than metric distance: Evidence from a field study.*, Proceedings of the national academy of sciences **105**(4), 1232–1237 (2008).
- [2] D. G. Shashi Thutupalli and R. Singh, *Boundaries determine the collective dynamics of self-propelled particles.*, PNAS (2018).
- [3] D. Geyer, *Du mouvement au blocage collectif dans les assemblees de rouleurs colloïdaux : hydrodynamique et solidification des liquides polaires actifs.*, Thèse de doctorat de l’université de Lyon (2019).
- [4] B. D. Bricard A., Caussin JB., *Emergence of macroscopic directed motion in populations of motile colloids.*, Nature **503**(7474), 95–98 (2013).
- [5] A. Bricard., *Dynamiques collectives de colloïdes auto-propulsés.*, PhD thesis, Université Paris Diderot (Paris 7) (2014).
- [6] N. Desreumaux., *Emulsions microfluidiques et rouleurs colloïdaux : effets collectifs en matière molle forcée hors-équilibre.*, PhD thesis, Université Pierre et Marie Curie (2015).
- [7] O. D. Julien Deseigne and H. Chate., *Collective motion of vibrated polar disks.*, Physical review letters **105**(9):098001 (2010).
- [8] C. S. E. F. Volker Schaller, Christoph Weber and A. R. Bausch., *Polar patterns of driven filaments.*, Nature **467**(7311):73 (2010).
- [9] J. Z. C. X. E. L. Jing Yan, Ming Han and S. Granick., *Reconfiguring active particles by electrostatic imbalance.*, Nature Materials **15**:1095 EP (2016).
- [10] T. Vicsek and A. Zafeiris., *Collective motion.*, Physics reports **517**(3-4), 71–140 (2012).
- [11] A. Morin, *Colloidal flocks in challenging environments.*, Soft Condensed Matter [cond-mat.soft] (2018).
- [12] J. Toner and Y. Tu., *Flocks, herds, and schools: A quantitative theory of flocking.*, Phys. Rev. E **58**:4828–4858 (1998).
- [13] G. Quincke., *Über Rotationen im constanten electrischen Felde.*, G. Ann. Phys. (1896).

-
- [14] J.-B. Caussin., *Dynamiques collectives de colloides auto-propulsés: ondes, vortex, essaim, tressage.*, PhD thesis, Ecole normale supérieure (2015).
 - [15] P. J. Lu., *Gelation and Phase Separation of Attractive Colloids.*, PhD thesis, Harvard University (2008).
 - [16] J. C. Crocker and D. Grier., *Methods of digital video microscopy for colloidal studies.*, Journal of Colloid and Interface Science - J COLLOID INTERFACE SCI **179:298–310** (1996).
 - [17] A. Chardac, *Matiere active et mouvements collectifs en milieux desordonnes*, Rapport de stage Master ICFP de l'Ecole Normale Supérieure (2018).
 - [18] J.-B. C. Antoine Bricard and D. Bartolo, *Emergent vortices in populations of colloidal rollers.*, Nature Communications (June 2015).